Dual-frequency dielectrophoretic levitation of *Canola* protoplasts

Karan V. I. S. Kaler,* Jing-Ping Xie,* Thomas B. Jones,‡ and Reginald Paul§

*Department of Electrical and Computer Engineering, University of Calgary, Calgary, Alberta, T2N 1N4 Canada; ‡Department of Electrical Engineering, University of Rochester, Rochester, New York 14627 USA; and §Department of Chemistry, University of Calgary, Calgary, Alberta, T2N 1N4 Canada

ABSTRACT A novel dual-frequency excitation technique is introduced which permits investigation of the low-frequency dispersion of *Canola* plant protoplasts using feedback-controlled dielectrophoretic levitation. The upper and intermediate frequency spectra obtained using the new technique are generally consistent with previous work. However, below some cross-over frequency f_{OL}, the protoplasts exhibit an apparent positive dielectrophoretic response that is not predicted by conventional theory. This cross-over frequency is linearly related to suspension conductivity, virtually independent of the suspension pH, and inversely proportional to the square of the cell radius. Examination of the complex Clausius-Mossotti polarization coefficient reveals that the observed positive dielectrophoretic response can not be accounted for in terms of Maxwell-Wagner polarization associated with a conventional layered model for the protoplast. The failure of straightforward enhancements to the protoplast model in explaining the low frequency behavior may indicate the presence of an electrophoretic contribution to the net observable force on the particle. To account for such fluid mechanical effects, it will be necessary to modify the existing dielectrophoretic force formulation.

INTRODUCTION

Dielectrophoretic (DEP) levitation has demonstrated value in measuring the frequency-dependent dielectric polarization of small particles and particle chains in the size range from ~5 μm to ~200 μm. An axisymmetric electrode structure producing a focussed electric field has been employed with feedback control to levitate metallic spheres (Jones and Kraybill, 1986; Tombs and Jones, 1991), model biological cells (Kaler and Jones, 1990), and other particles exhibiting a positive DEP effect. Electrodes producing a cusped electric field have been used to investigate droplets (Veas and Schaffer, 1969), bubbles (Jones and Bliss, 1977), and particles (Bahaj and Bailey, 1979) exhibiting negative dielectrophoresis. Live biological cells in aqueous suspension are examples of particles exhibiting both positive and negative DEP responses in different regions of the frequency spectrum (Marszalek et al., 1989). To date, however, DEP levitation of living cells has been restricted in its use to frequencies where cells exhibit only a positive DEP response. As a result, the advantages of feedback-controlled levitation have not yet been brought to bear in studies of the low-frequency behavior of cells, where negative dielectrophoresis usually reigns.

In this paper, we describe a summed dual-frequency feedback-controlled levitation method which circumvents the above limitation. We have used this new scheme to examine the positive and negative DEP spectra of *Canola* plant protoplasts over a considerably wider frequency range (from ~1 Hz to ~50 MHz) than previously reported. The results thus obtained are compared to the predictions of a standard cell model and it is found that the behavior at the lowest frequencies is inconsistent with theoretical predictions. The principal finding is an apparent positive DEP response at low frequencies which can not be accounted for by Maxwell-Wagner polarization or other relaxation processes one might associate with protoplasts. Because low frequency relaxation mechanisms intrinsic to the suspension medium can be ruled out, some additional force contribution must be sought in explanation of the anomalous behavior. The obvious candidate is electrophoresis, which is of well-known significance for cells in a DC electric field and may have an observable effect in the case of AC fields at frequencies below ~1 kHz.

THEORY

DEP levitation exploits the voltage-controllable force ($\bar{F}_{DEP}$) exerted by a nonuniform AC electric field upon a polarizable particle to counteract the net force due to gravity ($\bar{F}_g$). To achieve levitation, an equilibrium must be established between these two forces, that is

$$\bar{F}_{DEP} + \bar{F}_g = 0, \tag{1}$$

where the net gravitational force on a spherical particle of radius r of mass density γ_1 suspended in a fluid medium of mass density γ_2 is

$$\bar{F}_g = {}^4/_3\pi r^3(\gamma_2 - \gamma_1)\bar{g}. \tag{2}$$

In Eq. 2, $\bar{g}$ is the gravitational acceleration vector with magnitude $|\bar{g}| = g = 9.81$ m/s^2. Consistent with the theory of Sauer (1983), the time-average DEP force for a multilayered spherical shell characterized by complex permittivity $\underline{\epsilon}_{eff}$ and immersed in a medium of complex permittivity $\underline{\epsilon}_1$ may be expressed as

$$\langle \bar{F}_{DEP} \rangle = 2\pi r^3 \epsilon_1 \mathrm{Re}[\underline{K}_e]\nabla E^2, \tag{3}$$

where E is the magnitude of the externally applied electric field and $\underline{K}_e$, the well-known Clausius-Mossotti factor, is a measure of the excess effective polarizability of the particle.

0006-3495/92/07/058/12 $2.00

$$\underline{K}_e(\underline{\epsilon}_{eff}, \underline{\epsilon}_1) = \frac{\underline{\epsilon}_{eff} - \underline{\epsilon}_1}{\underline{\epsilon}_{eff} + 2\underline{\epsilon}_1}. \quad (4)$$

Here, $\underline{\epsilon}_{eff} = \epsilon_{eff} + \sigma_{eff}/j\omega$ and $\underline{\epsilon}_1 = \epsilon_1 + \sigma_1/j\omega$ are the complex permittivities of the particle and the suspension medium. The frequency-dependent quantities ϵ_{eff} and σ_{eff} are the apparent permittivity and conductivity of the particle, respectively, whereas ϵ_1 and σ_1 are the permittivity and conductivity of the suspension medium. Finally, ω is the electrical frequency in radians per second and $j = \sqrt{-1}$.

Under the condition of positive dielectrophoresis, that is, $\mathrm{Re}[\underline{K}_e] > 0$, the DEP force $\bar{F}_{DEP}$ attracts the particle into the region of maximum electric field intensity. On the other hand, when $\mathrm{Re}[\underline{K}_e] < 0$, the particle exhibits negative dielectrophoresis by being drawn into the region of minimum electric field intensity. Biological cells typically exhibit both positive and negative DEP responses in different regions of the frequency spectrum. Therefore, for broadband measurements on a biological cell using DEP levitation, we must resort to two distinctly different levitation schemes. For particles, droplets and bubbles exhibiting negative DEP, passive levitation using a cusped axisymmetric electric field must be employed, while for cells or particles exhibiting positive DEP, stable levitation is achievable only using a focussing electrode structure and feedback. In principle, one could make use of the passive and feedback-controlled levitation methods in two separate measurements to obtain, respectively, the negative and positive DEP portions of the spectrum. However, this approach is extremely inconvenient in single cell studies because considerable difficulty is encountered in calibration of the two different systems to quantify the DEP response. These calibration problems are particularly troublesome at low frequencies (<1 kHz), where electrode polarization effects become significant. Furthermore, excessive handling of individual cells is best avoided, due to the likelihood of their sustaining damage when being transferred between positive and negative DEP levitation chambers.

To circumvent these difficulties and still obtain both negative and positive DEP spectral data for individual plant protoplasts of *Canola,* we have modified an existing feedback controller to achieve particle levitation by the summation of two AC voltages at different frequencies. This dual frequency levitation scheme facilitates examination of both the positive and negative DEP responses of lone cells in one levitation chamber.

Single-frequency feedback-controlled levitation

Stable levitation of a particle experiencing a positive DEP force requires a focussed electric field to achieve radial stability and a feedback control scheme to control the axial location of the particle. Refer to Fig. 1 which depicts a focussed electric field created by axisymmetric

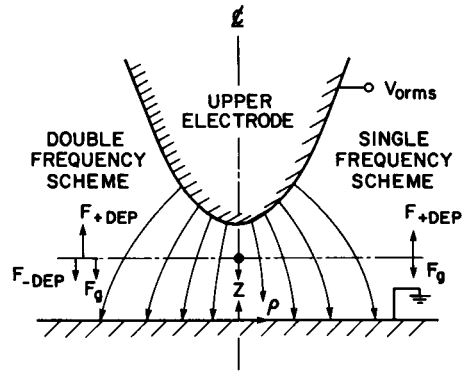

FIGURE 1 Cross-sectional view of the electrode geometry used in single-cell levitation experiments and comparison of the single and dual-frequency levitation schemes.

electrodes. In this system, the DEP force automatically centers the particle along the axis between the chamber electrodes and balances the downward-directed gravitational force. The equilibrium equation relating the dielectrophoretic and gravitational forces may be manipulated to obtain an expression for $\mathrm{Re}[\underline{K}_e]$ in terms of particle and field parameters. Combining Eqs. 1, 2, and 3, we obtain

$$\mathrm{Re}[\underline{K}_e(\omega)] = \frac{2|\gamma_2 - \gamma_1|g}{3\epsilon_1|\partial E^2/\partial z|}. \quad (5)$$

The axial field gradient term $|\partial E^2/\partial z|$ for the cone-plate electrode configuration of Fig. 1 is well-approximated by the following expression (Jones and Kraybill, 1986).

$$\frac{\partial E^2}{\partial z} = -\frac{16V_0^2\underline{z}}{h^3(1-\underline{z}^2)^3}\ln\left(\frac{1+\underline{z}_{min}}{1-\underline{z}_{min}}\right), \quad (6)$$

where V_0 is the voltage applied to the chamber electrodes, z_{min} is the on-axis electrode spacing, θ is the asymptotic cone angle of the upper electrode, and the following normalizations have been utilized: $\underline{z} = z/h$, $\underline{z}_{min} = z_{min}/h$, and $h = z_{min}/\cos(\theta/2)$.

The experimental technique is to adjust the voltage as the frequency is changed so as to maintain the particle at fixed position $\underline{z}$; in this way, the field gradient normalized to the voltage is held constant for all measurements. To quantify $\mathrm{Re}[\underline{K}_e]$ using Eq. 5, it is necessary to calibrate the electrodes or use Eq. 6. It is also necessary to determine the particle-medium density difference, $\gamma_2 - \gamma_1$, which may exhibit considerable variation within a population of biological cells. Note that important information about cell parameters is most readily accessible in the regions of the spectrum where the DEP response undergoes change, particularly zero-crossings.

DUAL-FREQUENCY FEEDBACK-CONTROLLED LEVITATION

If the frequency is changed so that $\mathrm{Re}[\underline{K}_e(\omega)]$ approaches zero, the voltage required to levitate a given particle in-

creases without bound; when $\mathrm{Re}[\underline{K}_e(\omega)]$ goes negative, single-frequency active feedback control using the electrodes shown in Fig. 1 fails to maintain the particle in stable equilibrium on axis. This is because the focussed electrostatic field configuration can no longer sustain radial stability. Therefore, to perform measurements when $\mathrm{Re}[\underline{K}_e] < 0$ with the focussed field electrode structure and feedback-control, the dual-frequency technique must be exploited.

Under dual-frequency excitation, the net electric field acting on the levitated particle consists of two components E_1 and E_2 produced by the summation of two AC voltages at distinct frequencies ω_1 and ω_2. By convention, we will assume here that ω_1 is the test frequency at which all spectra are measured, so that $\omega_1 < \omega_2$.

$$V_{net}(t) = V_1 \cos(\omega_1 t + \phi) + V_2 \cos(\omega_2 t), \quad (7)$$

where ϕ is an arbitrary phase factor. V_1 is fixed, ω_1 is the variable scanning frequency, V_2 is the feedback-controlled, amplitude-modulated voltage, and ω_2 is fixed at a value where $\mathrm{Re}[\underline{K}_e]$ is positive and essentially constant with frequency.

For dual frequency excitation, calculation of the net dielectrophoretic force is complicated by the fact that the force depends upon the electric field squared. Nevertheless, it may be shown that the net time-average DEP force can be expressed as the sum of two terms, each in the form of Eq. 3.

$$\langle \bar{\mathbf{F}}_{DEP} \rangle_{net} = \langle \bar{\mathbf{F}}_{DEP} \rangle_{\omega_1} + \langle \bar{\mathbf{F}}_{DEP} \rangle_{\omega_2}. \quad (8)$$

Eq. 8 may be used in analysis of data obtained with the DEP levitator, provided that sufficient time is spent performing the measurement at each frequency to insure that the controller has reached equilibrium. This consideration becomes very important because, due to the tedious and time-consuming nature of gathering data, all experimental runs with the levitator are automated and the shortest possible time interval is spent making each measurement before the frequency is changed to the next value. It is shown in Appendix A that, if the two electric field frequencies ω_1 and ω_2 are widely separated (that is, $\omega_1 \ll \omega_2$) and if the time interval for each measurement is sufficiently long, then equilibrium is assured in the measurements and the expression for net time-average DEP force can be represented accurately by Eq. 8.

The simple force addition expression is exploited in the feedback-controlled DEP levitator to investigate the negative spectra of individual biological cells. First, assume that the unknown quantity $\mathrm{Re}[\underline{K}_e(\omega_1)]$ is to be measured, while $\mathrm{Re}[\underline{K}_e(\omega_2)] > 0$ has been determined by means of an initial calibration step. The calibration step can be represented in terms of the balance of the gravitational and DEP forces with only $V_2 = V_{cal}$ applied, that is,

$$F_g = \langle F_{DEP} \rangle \propto \mathrm{Re}[\underline{K}_e(\omega_2)] V_{cal}^2, \quad (9)$$

where V_{cal} is the calibration voltage. As long as the +DEP force term in Eq. 8 dominates, the particle can be stably maintained in the levitator and the desired measurements can be performed. If $\mathrm{Re}[\underline{K}_e(\omega_2)]$ is already known, then the change in V_2 required to maintain the particle at fixed position when V_1 is added will provide an indirect measure of $\mathrm{Re}[\underline{K}_e(\omega_1)]$.

In the conduct of a typical experimental measurement performed upon a protoplast, ω_1 is usually initialized at a value where +DEP reigns. Then, ω_1 is lowered until $\mathrm{Re}[\underline{K}_e(\omega_1)]$ goes to zero and becomes negative. As ω_1 is changed, the feedback controller adjusts V_2 to achieve stable levitation at some fixed point in the chamber. The condition of equilibrium under dual frequency excitation can be expressed in terms of an initial calibration step.

$$\mathrm{Re}[\underline{K}_e(\omega_1)] V_1^2 + \mathrm{Re}[\underline{K}_e(\omega_2)] V_2^2 = \mathrm{Re}[\underline{K}_e(\omega_2)] V_{cal}^2. \quad (10)$$

Then, Eq. 10 is manipulated into a form from which the unknown low frequency DEP spectrum, $\mathrm{Re}[\underline{K}_e(\omega_1)]$, can be extracted.

$$\mathrm{Re}[\underline{K}_e(\omega_1)] = \mathrm{Re}[\underline{K}_e(\omega_2)] \left(\frac{V_{cal}^2 - V_2^2}{V_1^2} \right). \quad (11)$$

It is noteworthy that the dual frequency scheme described above is not limited to measurements at frequencies where $\mathrm{Re}[\underline{K}_e(\omega_1)]$ is negative, but may be used just as effectively in regions on either side of the zero-crossing, that is, when the magnitude of $\mathrm{Re}[\underline{K}_e(\omega_1)]$ is small. This feature is particularly valuable because of the inherent attractiveness of null detection as a measurement strategy. Such nulls, defined by the condition $\mathrm{Re}[\underline{K}_e(\omega)] = 0$, exist at any frequency such that $V_2 = V_{cal}$.

Levitation system

The dual-frequency levitation system, shown in Fig. 2, is identical in all respects to our original system (Kaler and Jones, 1990) except for the addition of a second programmable AC signal generator, a wide-band electronic summing amplifier, and some modifications to the controller software. The chamber, shown in sectional view in the same figure, consists of gold-plated stainless steel, cone-plate electrodes (with $z_{min} = 450$ μm and $\theta = 60$ deg) housed in an acrylic plastic chamber. Gold-plated electrodes are found superior to polished stainless steel in reproducibly minimizing significant electrode polarization effects encountered at low frequencies. Electrode polarization reduces the effective value of the field experienced by cells in the levitation chamber; therefore, to get accurate results, a frequency-dependent correction relating the applied voltage to the actual electric field is essential. To obtain this correction factor, we measured the characteristic impedance of the chamber over a wide range of frequencies and suspension conductivities. The complication of non-linearity was avoided by performing all the impedance measurements on the cell at the same signal strengths used in the levitation experiments. These data were used to calculate the ratio of the elec-

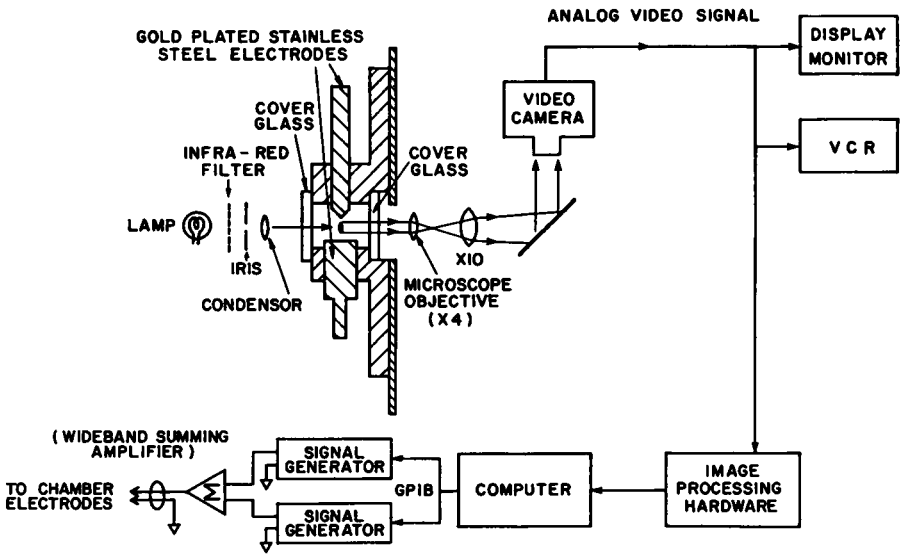

FIGURE 2 Sectional view of the levitation chamber showing the focussing electrode structure and also showing a block diagram of the dual-frequency levitation hardware.

trode impedance to the medium impedance, as shown in Fig. 3. At lower frequencies in the more conductive suspension media, the correction factor is quite large.

The chamber is loaded with a dilute suspension containing cells and mounted upon a vertical microscope stage. A video camera coupled to the microscope optics obtains an image of the cell which is used to monitor the cell location continuously for use by the servo control system. The video camera also makes possible visual examination of all levitated cells. The computer-controlled servo system is programmed to maintain levitated cells fixed at a pre-determined location between the chamber electrodes. For these small cells, it is our experience that a simple "proportional + integral" (PI) feedback control algorithm is adequate for reliable levitation. The magnitude of voltage V_2 applied to the electrodes during the time interval $nT < t < (n + 1)T$ is based on the detected location of the cell.

$$V_2(nT) = G_p e(nT) + G_i \sum_{k=1}^{k=n-1} e(kT), \qquad (12)$$

where n is the time index, k is the sample number, T is the sample interval and $e(nT)$ is the cell position error detected by the controller. G_p and G_i, respectively, the

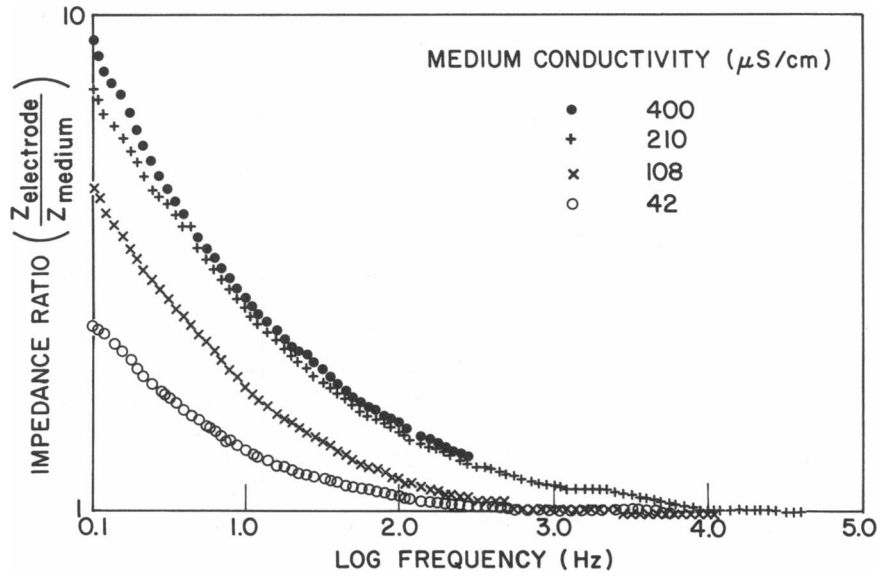

FIGURE 3 Plot showing the ratio of electrode polarization impedance to the suspension medium impedance versus frequency for a range of conductivity values. All solutions are adjusted to constant pH = 5.5.

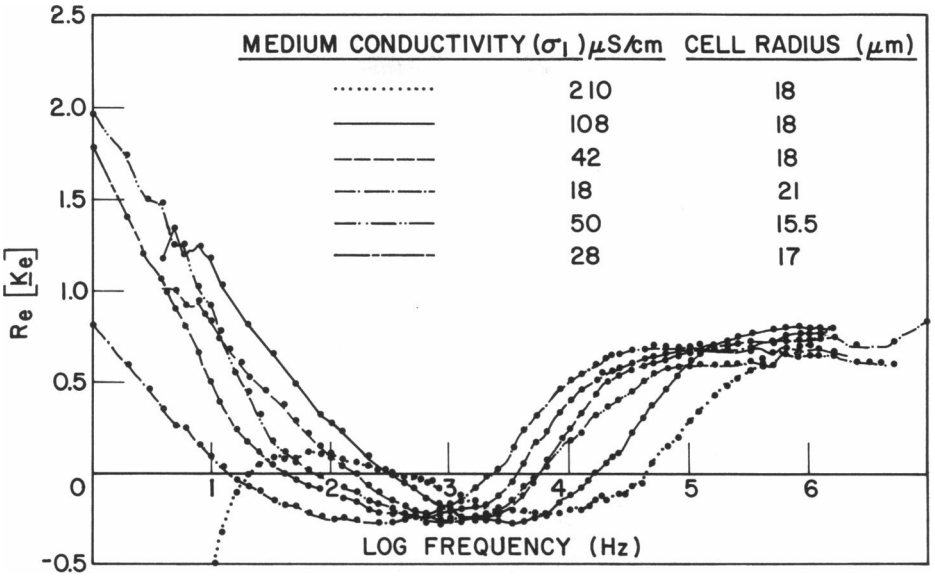

FIGURE 4 DEP spectra (Re[$\underline{K}_e$] versus frequency) for *Canola* protoplasts suspended in 8% sorbitol solution of varied electrical conductivity σ_1 with constant pH = 5.9. The dual-frequency method was used to obtain these data. Upper and lower zero-crossings in these spectra are referred to as f_{OH} and f_{OL}, respectively, in the text.

proportional and integral gain constants, are user-adjustable in real time for robust control action.

SAMPLE PREPARATION

The *Canola* plant protoplasts used in the investigation are prepared for experimental measurement in the levitator using an enzymatic digestion protocol described earlier (Kaler and Jones, 1990). The conductivity of the dilute cell suspension (σ_1) is adjusted by the addition of KCl and then monitored by a conductivity meter (model #1710, Bio-Rad Laboratories, Richmond, CA.). MES and TRIS buffers are used to control and vary suspension pH; this important parameter was monitored using a pH meter (Accumet, model #620, Fisher Scientific, Pittsburgh, PA.).

RESULTS

All measurements are carried out near 22°C using *Canola* plant protoplasts, suspended in 8% sorbitol solutions with conductivity (σ_1) and pH values ranged from 18 to 210 μS/cm and 4.6 to 8.0, respectively. Typical data, obtained using a combination of single- and dual-frequency methods, are shown in Figs. 4 and 5. In the first of these plots, the effective polarizability Re[$\underline{K}_e(\omega_1)$] is plotted versus frequency for solutions of varied electrical conductivity. These DEP spectra display strong sensitivity to σ_1 at frequencies below approximately 1 MHz. Fig. 5 shows additional DEP spectra obtained for protoplasts of several different radii but with σ_1 held constant. One common feature of all these spectra is the existence of a region of negative dielectrophoresis marked by two zero-crossings: ω_{OL} at the low-frequency end and ω_{OH} at the high-frequency end.

We have shown previously that the positive DEP response in the intermediate frequency region of the spectrum can be predicted successfully by the following approximate expression for the Clausius-Mossotti function (Kaler and Jones, 1990):

$$\underline{K}_e \cong \frac{j\omega(\tau'_m - \tau_1 - \tau_m) - 1}{j\omega(\tau'_m + 2\tau_1 + 2\tau_m) + 2}, \tag{13}$$

where $\tau'_m = c_m r/\sigma_1$, $\tau_m = c_m r/\sigma_3$, and $\tau_1 = \epsilon_1/\sigma_1$. Here, c_m is the capacitance per unit area of the cell membrane, r is the cell radius, ϵ_1 is the suspending medium permittivity, while σ_1 and σ_3 are the ohmic conductivities of the suspending medium and cell interior (cytoplasm), respectively. Eq. 13 ignores the influence of finite membrane transconductance, membrane charging, and surface conductivity. From Eq. 1, the DEP spectrum is related to the real part of the polarizability $\underline{K}_e(\omega)$.

$$\text{Re}[\underline{K}_e] = \frac{c_m r - \epsilon_1}{c_m r + 2\epsilon_1}\left[\frac{\omega^2 - 2/\tau_a\tau_b}{\omega^2 + 4/\tau_b^2}\right], \tag{14}$$

where the following time constants are defined: $\tau_a = \tau'_m - \tau_1 - \tau_m$ and $\tau_b = \tau'_m + 2\tau_1 + 2\tau_m$.

Estimates for c_m may be obtained by examining the effect of changing the suspension conductivity σ_1 upon the corner or 3 dB frequency. Using the dual-frequency method, this same information becomes much more readily available by a simple null detection approach, that is, by determining the frequency ω_{OH} such that Re[$\underline{K}_e$] = 0. From Eq. 14, we may derive

$$\omega_{OH} = \sqrt{\frac{2}{\tau_a\tau_b}}. \tag{15}$$

Typically, $\tau'_m \gg \tau_1$ and $\tau'_m \gg \tau_m$, so that Eq. 15 is quite well-approximated by the following expression.

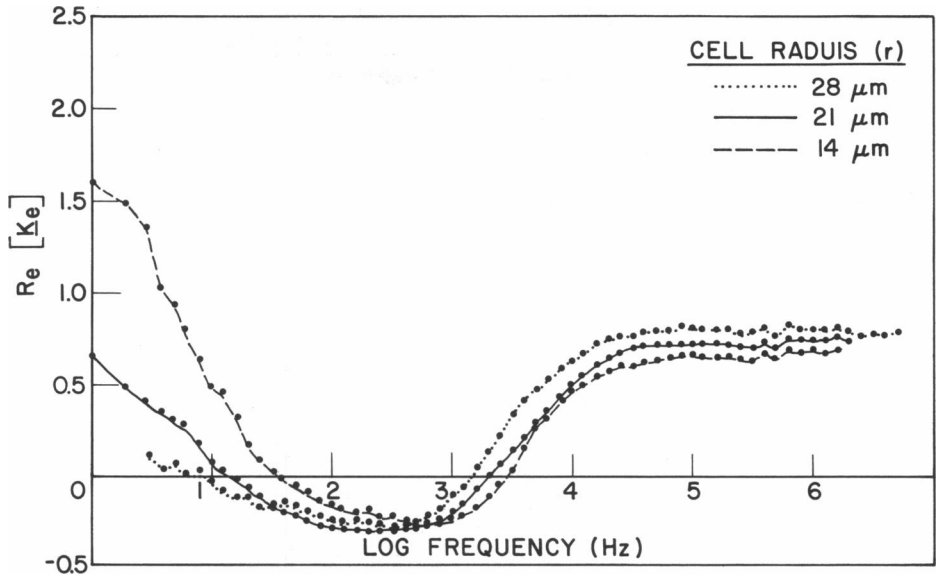

FIGURE 5 DEP spectra of *Canola* protoplasts for a range of cell radii (r) suspended in 8% sorbitol solution with conductivity σ_1 = 18 μS/cm and pH = 5.88.

$$\omega_{OH} \cong \frac{\sqrt{2}}{\tau'_m} = \frac{\sqrt{2}\sigma_1}{rc_m} \tag{16}$$

When the product of measured cell radius and cross-over frequency, $rf_{OH} = r\omega_{OH}/2\pi$, is plotted versus suspension conductivity σ_1, a straight line is obtained, the slope of which is inversely related to the membrane capacitance. Refer to Fig. 6. From a linear regression analysis of these data, we obtain the result c_m = 0.48 ± 0.1 μF/cm², in good agreement with 0.47 ± 0.1 μF/cm² obtained from an analysis of the 3 dB point on the positive DEP spectra of identical protoplasts (Kaler and Jones, 1990).

Below ω_{OH}, the polarization spectra for *Canola* protoplasts deviate quite significantly from the predictions of the simple protoplast model upon which Eq. 13 is based. First of all, the model predicts that Re[$\underline{K}_e$] should approach a steady conductivity-controlled value as $\omega \to 0$ (which will be equal to −0.5 if the effective conductivity of the cell is much lower than the suspension medium, that is, $\sigma_{eff} \ll \sigma_1$). However, examinations of the spectra in Figs. 4 and 5 reveal that, in the region of negative DEP, Re[$\underline{K}_e$] ≈ −0.3 and then only maintains this minimum value over a limited frequency range. Such a result certainly implies that σ_{eff} is smaller than σ_1 because the particle does exhibit negative dielectrophoresis. However, Re[$\underline{K}_e$] never settles to a value of −0.5, suggesting that either finite transmembrane conductance or effective surface conductivity (Chizmadzhev et al., 1985) allows σ_{eff} to remain appreciable compared to σ_1. This negative DEP response is consistent with that reported for single *Neurospora rassa* (slime mold) cells by Marszalek et al. (1989) who used a dynamic dielectrophoresis technique.

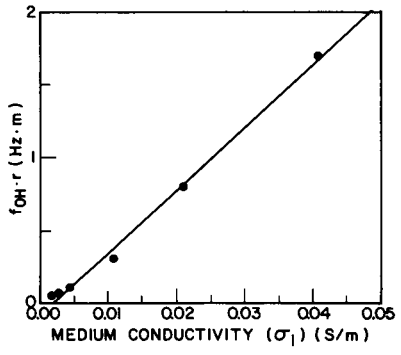

FIGURE 6 Dependence of the product of cell radius (r) and measured DEP cross-over frequency (f_{OH}) upon suspension conductivity σ_1. The slope of this plot is used with Eq. 16 to estimate the cell membrane capacitance c_m. For the data shown, linear regression for the slope gives the result c_m = 0.48 ± 0.01 μF/cm².

Low frequency behavior

The really significant departure of the experimental data from predictions of the simple protoplast model becomes evident when the test frequency ω_1 is further decreased. At these very low frequencies, Re[$\underline{K}_e$] goes through a second zero-crossing (at $\omega_1 = \omega_{OL}$) and becomes positive again. Burt et al. (1990) report a similar positive DEP response at comparable frequencies using a distinctly different measurement method. Note that, especially for some of the higher conductivity values, Re[$\underline{K}_e$] ≥ 1, which is not allowed according to the definition of the Clausius-Mossotti function. Electrode polarization can not be the cause of this anomaly; electrode polarization would tend to depress the estimated value for Re[$\underline{K}_e$].

Fig. 7 contains a plot of $r^2 f_{OL} = r^2\omega_{OL}/2\pi$, the measured low-frequency zero-crossing multiplied by the

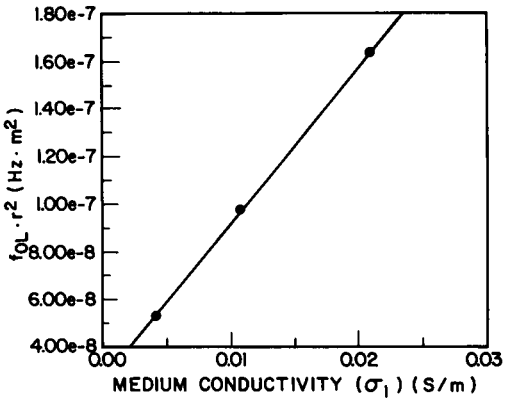

FIGURE 7 Dependence of the product of cell radius squared (r^2) and measured low-frequency DEP cross-over (f_{OL}) upon suspension conductivity σ_1.

square of the cell radius versus the suspension conductivity σ_1. That this correlation is moderately successful may mean that some surface polarization mechanism consistent with Schwarz (1962) is important. However, the positive DEP response at the lowest frequencies remains without explanation.

The protoplast model's failure to predict DEP spectra at low frequencies forces us to re-examine all the inherent or stated approximations in order to develop one or more hypotheses which may lead to an improved model. In Appendix B, we have examined the frequency-dependent behavior of the Clausius-Mossotti function $\underline{K}_e(\underline{\epsilon}_{eff}, \underline{\epsilon}_1)$ by inserting into this function various realizable complex permittivity expressions for the layered particle permittivity $\underline{\epsilon}_{eff}$ and the suspension medium permittivity $\underline{\epsilon}_1$ and then searching for any general rules for the allowed frequency dependence of Re[$\underline{K}_e$]. The most important outcome of this exercise is that a protoplast, suspended in an ohmic medium with no significant relaxation mechanism(s) in the frequency range from ~1 Hz to ~1 MHz, can not exhibit positive dielectrophoresis at the lowest frequencies while still exhibiting the conductivity-dominated negative DEP at intermediate frequencies and the membrane-capacitance-dominated positive DEP at higher frequencies. Because we do not expect our aqueous sorbitol cell suspension media to exhibit a significant dielectric relaxation in this frequency range, we conclude that the observed positive DEP response of protoplasts at low frequencies is inconsistent with conventional dielectrophoretic theory.

It is tempting to propose more elaborate models for the protoplast with additional relaxation processes. Indeed, many enhanced models for cells and colloidal particles have been proposed in the past, such as protoplasts containing chloroplasts (Gimsa et al., 1991), colloidal particles with counter-ion cloud layers (Schwarz, 1962; Schurr, 1964), as well as various multilayered shells with multiple Maxwell-Wagner polarization mechanisms. Nevertheless, the conclusion of Appendix B, that positive DEP at the lowest measured frequencies is impossible for a protoplast in an aqueous suspension medium, remains unchanged. Such a result, that the addition of more relaxation processes or more layers to the cell model can never explain the positive DEP at low frequencies, leads us to suspect that there is a serious breakdown of the force calculation model itself.

A possible explanation for the anomalous behavior observed is electrophoresis. If the membrane is naturally charged, significant electric-field-induced motions of the counter-ion charges in the diffuse double-layer surrounding the cell might be expected if the imposed electric field frequency is sufficiently low. If electrophoretic motion is present, then the conventional calculation of the net force on the cell based upon the dielectrophoretic theory is incomplete. Such an hypothesis is not new (Foster et al., 1992). Furthermore, possibly related anomalous electrorotational behavior of colloidal particles has been reported at low frequencies by Arnold et al. (1987).

pH sensitivity

In addition to the effects of cell radius r and suspension conductivity σ_1, we have also examined the influence of pH on the polarization response. Refer to the DEP spectra shown in Fig. 8 which indicate that the magnitude of the apparent positive DEP effect at low frequency is quite sensitive to pH. On the other hand, neither the low ($f_{OL} = \omega_{OL}/2\pi$) nor the middle frequency ($f_{OH} = \omega_{OH}/2\pi$) cross-overs are affected. Such results are at least consistent with the hypothesis that electrophoresis is responsible for the low frequency behavior. Phosphate (Obi et al., 1989), carboxylate (Nagata and Melchers, 1978) and amino groups (Morikawa et al., 1982) are the principal charged groups on the surface of plant protoplasts (Senn and Pilet, 1981). When pH is increased, the phosphate and carboxylate charge groups increase the negative surface charge density and the counter-ion cloud concentra-

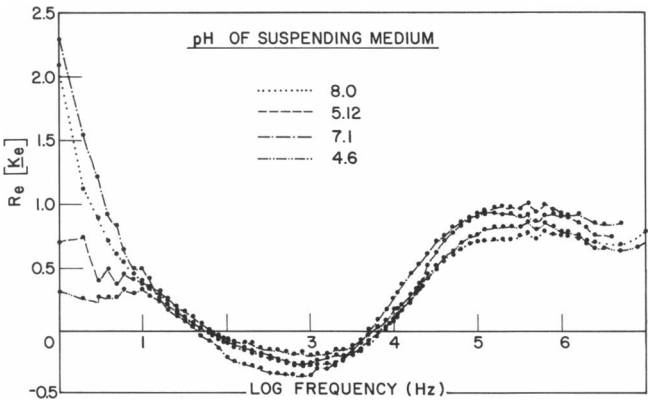

FIGURE 8 The influence of cell medium pH upon the dielectrophoretic spectra of *Canola* protoplasts with the medium conductivity σ_1 adjusted to 45 μS/cm and the cell radius $r \approx 18$ μm.

tion, reducing the number of scattering sites. The consequence of this interfacial charge redistribution could be an increase in the apparent surface conductivity which would give rise to increased Re[$\underline{K}_e$] as pH is increased. A marked dependence upon pH is observed for the low-frequency membrane capacitance of *Chara cerallina* cells by Coster and Smith (1974), who found that the measured membrane capacitance at frequencies below 4 Hz and pH $\sim$ 9 is much larger than at pH $\sim$ 5.5.

CONCLUSION

This article reports the first successful use of a new dual frequency feedback-controlled levitation scheme to obtain both the positive and negative DEP spectra of lone plant protoplasts in a single measurement apparatus. With this method, it is possible to investigate the dielectric responses of living biological cells over the very wide spectral range from $\sim$1 Hz to $\sim$1 MHz. The intermediate and high-frequency data thus obtained generally conform to the expectations of a simple spherical protoplast model (Kaler and Jones, 1990). A zero-crossing of the DEP spectrum is used to obtain an estimate of the membrane capacitance, $c_m = 0.48 \pm 0.01$ μF/cm^2, which is in good agreement with previous measurements upon the same type of protoplast.

Unlike the high and intermediate frequency regions of the DEP spectrum, the low frequency data reveal characteristics which depart significantly from the idealized protoplast model. The principal departure is an apparent, very pronounced positive DEP effect at the lowest frequencies. The authenticity of this effect as a dielectrophoretic response must be questioned on two fundamental bases: (*a*) Re[$\underline{K}_e$] > 1, which is disallowed based on the definition of $\underline{K}_e$, and (*b*) the unrealizable nature of positive DEP at the lowest frequencies subject to reasonable assumptions about the suspension medium. In fact, it is not possible to construct a protoplast model from physically realizable building blocks (e.g., thin capacitive or resistive layers, finite layers, or layers with intrinsic Debye-like relaxation mechanisms) which exhibits positive DEP at low frequencies unless the suspension medium itself exhibits dielectric relaxation.

The generally accepted theory for electrophoresis (cf O'Brien and White, 1978) relates particle motion $\bar{\mathbf{u}}$ directly to a uniform DC electric field vector $\bar{\mathbf{E}}_{DC}$, that is, $\bar{\mathbf{u}} \propto \bar{\mathbf{E}}_{DC}$. In accordance with this theory, the time-average, electrophoretic force on a stationary, levitated particle using an AC electric field would be zero. However, conventional electrophoretic models do not account for the significant nonuniformity of the electric field in a levitator. We suspect that, for frequencies below approximately 100 Hz, electrophoretic fluid motion masks—or even overwhelms—the dielectrophoretic force on protoplasts in aqueous suspension. Surface charging creates a counter-ion cloud extending from the cell surface approximately one Debye screening length into the fluid. The fluid in this layer experiences a body force when acted upon by the AC electric field. At sufficiently low frequencies, the fluid can respond to this force, leading to localized, time-varying flow close to the membrane surface. Such electrophoretic motions are not taken into account by dielectrophoretic theory.

Consistent with the electrophoresis hypothesis, the cells would have net particle charge on the surface; furthermore, if this surface charge were irregularly distributed on the membrane, the particle would have a permanent dipole moment. However, it may be shown readily that a particle with either fixed, net charge or a permanent dipole moment subjected to a nonuniform AC electric field experiences an additional force that emulates negative DEP. This is true irrespective of the sign of the charge or the moment. Therefore, the fixed charge can not in itself explain our results because the low-frequency effect we describe acts like positive DEP.

A new theory combining conventional dielectrophoretic and electrophoretic phenomena for nonuniform, AC electric fields at low frequencies is required. One observation that might serve as a starting point for a new theory is that the calculated Debye length is three orders of magnitude smaller than the plant protoplast radii over the entire range of KCl concentrations used in our experiments. In any case, it seems clear that the lack of a suitable low-frequency force calculation model complicate prediction of certain experimental phenomena and possibly hinders the investigation of some important membrane functions.

APPENDIX A

Dual frequency analysis

Eq. 8 provides an expression for the net dielectrophoretic force averaged over a long period of time that is exerted by an electric field comprised of two distinct AC components at frequencies ω_1 and ω_2. For measurements carried out over an extended period of time, this average force determines the equilibrium. However, when automated measurements are being made by the computer over a large frequency range, it becomes a practical matter to shorten the time interval T_s devoted to each frequency measurement in order to reduce the total time required to obtain the spectrum for a given cell. Minimizing the time required per measurement is especially important because protoplasts are very sensitive both to heat and to strong electric fields. Thus, subject to the restriction that each measurement is made at a true equilibrium, the time interval must be kept as short as possible. In the case of dual frequency excitation, very low frequencies are used (down to $\sim$1 Hz) and it is absolutely necessary to insure that equilibrium has been achieved before moving to the next frequency.

A numerical examination of this problem has been undertaken to determine if the sample interval used ($T_s \geq 5$ s) is adequate to insure this equilibrium. Consider the sum of two voltage signals $V_1(t)$ and $V_2(t)$ with frequencies ω_1 and ω_2 and one arbitrary phase factor ϕ, as defined by Eq. 7. We can determine if equilibrium is achieved by examining the value of the following integral:

$$V_{avg}^2 = \frac{1}{T_s}\int_0^{T_s} [V_1 \cos(\omega_1 t + \phi) + V_2 \cos(\omega_2 t)]^2 \, dt, \quad \text{(A1)}$$

where T_s is the time interval per measurement at a given frequency, a quantity that can be specified in the master program that runs the experiment. If T_s is too short, then the servo controller will not have had time to settle to its equilibrium and the measurement of Re[$\underline{K}_e(\omega)$]

will be inaccurate. We can easily determine if T_s is long enough by a numerical evaluation of A1 and a comparison to the sum of the two integrals:

$$(V_1^2)_{avg} = \frac{1}{T_s}\int_0^{T_s} [V_1 \cos(\omega_1 t + \phi)]^2\, dt, \qquad (A2)$$

and

$$(V_2^2)_{avg} = \frac{1}{T_s}\int_0^{T_s} [V_2 \cos(\omega_2 t)]^2\, dt. \qquad (A3)$$

The percent error is defined

$$\%\ \text{error} = \frac{V_{avg}^2 - [(V_1^2)_{avg} + (V_2^2)_{avg}]}{V_{avg}^2} \times 100. \qquad (A4)$$

Such a computation has been carried out for the following conditions:

$$V_1 = V_2,$$
$$T = 5\ \text{s},$$
$$1\ \text{Hz} \le f_1 = \omega_1/2\pi \le 1\ \text{MHz}$$
$$f_2 = \omega_2/2\pi = 1\ \text{MHz} \quad \text{(constant)}$$
$$0 \le \phi \le \pi/2\ \text{radians}.$$

It is found that the % error is negligible except when the phase difference and/or frequency difference between the two fields is very small. Because the condition $\omega_1 \ll \omega_2$ is maintained in all DEP levitation experiments, the sampling interval $T_s = 5$ s presents no loss of accuracy.

APPENDIX B

Realizable behavior of Clausius-Mossotti function for particle in suspension media

The limitation of physical realizability imposes certain restrictions upon the frequency-dependent dielectrophoretic response of particles suspended in liquid media. In this appendix, we focus on the set of restrictions that apply at low frequencies for the specific case of protoplasts suspended in aqueous media. The starting point is a set of general assumptions about modeling conductive and dielectric behavior in the suspension medium and in the cell: (*a*) The charge conduction mechanisms in the cell and in the suspension medium are linear and ohmic, characterized by conductivities σ_1 and σ_2. (*b*) All dielectric behavior is linear and characterized by one (or more) simple, first-order relaxations of the Debye type. Dielectric resonances are not considered; therefore, in accordance with the Debye model, the real part of the permittivity is a monotonically decreasing function of frequency ω. (*c*) Cells are modeled as structures consisting of concentric spherical shells and the media comprising the layers are lossy dielectrics with ohmic conduction as described in (*a*) and (*b*) above. (*d*) The frequency-dependent complex Clausius-Mossotti function ($\underline{K}_e$) represents the effective excess polarization of the suspended cell and may be used to determine the time-average DEP force and the electrical torque. Electrophoretic and electrohydrodynamical motions are not included in this model. The first two assumptions are widely accepted in modeling most DEP and electrorotation phenomena. Though it is likely that dielectric resonances may come into play at very high frequencies (>100 MHz), our neglect of dielectric resonance seems fully justified in the present case because of the focus on the anomalous behavior observed at very low frequencies (<1 kHz). The third assumption is quite appropriate because, for the purposes of examining the allowable low frequency DEP response, no loss of generality is sustained by restricting attention to spheres. The fourth assumption is consistent with the conventional electrostatic theory of dielectrophoresis.

A set of rules for the frequency-dependent behavior of the complex Clausius-Mossotti function $\underline{K}_e$, given by Eq. 4, may be deduced by considering the situation of a particle with complex dielectric permittivity $\underline{\epsilon}_2(\omega)$ in a suspension medium of permittivity $\underline{\epsilon}_1(\omega)$. Several illuminating cases are considered below.

Pure Debye model

Assume that the dielectric behavior for the particle and the suspension medium can be represented by the Debye equation and that DC conduction is negligible. Then,

$$\underline{\epsilon}_1 = \epsilon_\infty^1 + \frac{\epsilon_0^1 - \epsilon_\infty^1}{1 + j\omega\tau_1} \quad \text{and} \quad \underline{\epsilon}_2 = \epsilon_\infty^2 + \frac{\epsilon_0^2 - \epsilon_\infty^2}{1 + j\omega\tau_2}, \qquad (B1)$$

where τ_1 and τ_2 are the time constants associated with intrinsic relaxation processes in the suspension medium and the particle, respectively. The realizability condition on passive (lossy) dielectric media dictates that $\epsilon_0^1 > \epsilon_\infty^1$ and $\epsilon_0^2 > \epsilon_\infty^2$. Note that the expression for the effective permittivity of a protoplast with an insulating membrane is identical in form to Eq. B1 for $\underline{\epsilon}_2$ (Kaler and Jones, 1990). Using Eq. B1 in Eq. 4, the Clausius-Mossotti function may be written

$$\underline{K}_e = K_\infty \frac{\dfrac{1}{\tau_1\tau_2}\left(\dfrac{\epsilon_0^2 - \epsilon_0^1}{\epsilon_\infty^2 - \epsilon_\infty^1}\right) + j\omega\left[\dfrac{1}{\tau_1}\left(\dfrac{\epsilon_\infty^2 - \epsilon_0^1}{\epsilon_\infty^2 - \epsilon_\infty^1}\right) + \dfrac{1}{\tau_2}\left(\dfrac{\epsilon_0^2 - \epsilon_\infty^1}{\epsilon_\infty^2 - \epsilon_\infty^1}\right)\right] - \omega^2}{\dfrac{1}{\tau_1\tau_2}\left(\dfrac{\epsilon_0^2 + 2\epsilon_0^1}{\epsilon_\infty^2 + 2\epsilon_\infty^1}\right) + j\omega\left[\dfrac{1}{\tau_1}\left(\dfrac{\epsilon_\infty^2 + 2\epsilon_0^1}{\epsilon_\infty^2 + 2\epsilon_\infty^1}\right) + \dfrac{1}{\tau_2}\left(\dfrac{\epsilon_0^2 + 2\epsilon_\infty^1}{\epsilon_\infty^2 + 2\epsilon_\infty^1}\right)\right] - \omega^2}, \qquad (B2)$$

where K_0 and K_∞ are, respectively, the low and high frequency limits of $\underline{K}_e(\omega)$.

$$K_e|_{\omega\to 0} = K_0 \equiv \frac{\epsilon_0^2 - \epsilon_0^1}{\epsilon_0^2 + 2\epsilon_0^1} \quad \text{and}$$
$$K_e|_{\omega\to\infty} = K_\infty \equiv \frac{\epsilon_\infty^2 - \epsilon_\infty^1}{\epsilon_\infty^2 + 2\epsilon_\infty^1}. \qquad (B3)$$

The frequency-dependence of $\underline{K}_e$ can be most easily visualized by assuming that the dielectric relaxations are widely separated in the frequency domain. The two limiting cases are (a) $\tau_1 \ll \tau_2$ and (b) $\tau_1 \gg \tau_2$ and they are distinguished only by their behavior at intermediate frequencies. Numerical studies confirm the generality of the conclusions derived from these limiting cases.

(*case a*): $\tau_1 \ll \tau_2$

$$(\underline{K}_e)_{intermediate} \approx \left(\frac{\epsilon_\infty^2 - \epsilon_0^1}{\epsilon_\infty^2 + 2\epsilon_0^1}\right) \quad \text{for}$$
$$\frac{1}{\tau_2}\left(\frac{\epsilon_0^2 + 2\epsilon_0^1}{\epsilon_\infty^2 + 2\epsilon_0^1}\right) \gg \omega \gg \frac{1}{\tau_1}\left(\frac{\epsilon_\infty^2 + 2\epsilon_0^1}{\epsilon_\infty^2 + 2\epsilon_\infty^1}\right); \qquad (B4)$$

(*case b*): $\tau_1 \gg \tau_2$

$$(\underline{K}_e)_{intermediate} \approx \left(\frac{\epsilon_0^2 - \epsilon_\infty^1}{\epsilon_0^2 + 2\epsilon_\infty^1}\right) \quad \text{for}$$
$$\frac{1}{\tau_1}\left(\frac{\epsilon_0^2 + 2\epsilon_0^1}{\epsilon_0^2 + 2\epsilon_\infty^1}\right) \gg \omega \gg \frac{1}{\tau_2}\left(\frac{\epsilon_0^2 + 2\epsilon_\infty^1}{\epsilon_\infty^2 + 2\epsilon_\infty^1}\right). \qquad (B5)$$

In *case a*, $\mathrm{Re}[\underline{K}_e]$ must first decrease and then increase, while in *case b*, $\mathrm{Re}[\underline{K}_e]$ first increases and then decreases. This frequency-dependent

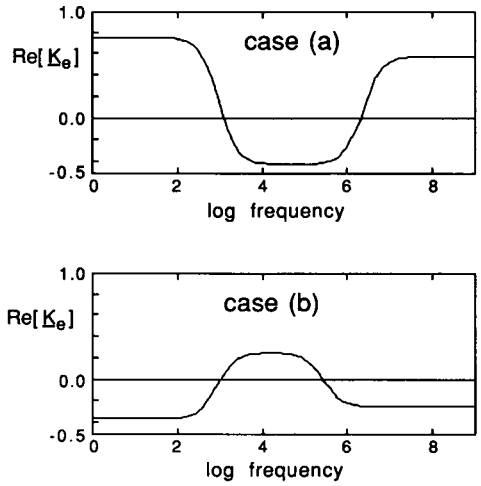

FIGURE B1 DEP spectrum for a lossy particle in a lossy suspension medium with no DC conduction. (*a*) $\tau_1 \ll \tau_2$: $\epsilon_0^1/\epsilon_0 = 100.0$, $\epsilon_\infty^1/\epsilon_0 = 2.0$, $\sigma_1 = 0.0$, $\tau_1 = 10^{-6}$ s; $\epsilon_0^2/\epsilon_0 = 1000.0$, $\epsilon_\infty^2/\epsilon_0 = 10.0$, $\sigma_2 = 0.0$, $\tau_2 = 10^{-3}$ s. (*b*) $\tau_2 \ll \tau_1$: $\epsilon_0^1/\epsilon_0 = 500.0$, $\epsilon_\infty^1/\epsilon_0 = 50.0$, $\sigma_1 = 0.0$, $\tau_1 = 10^{-3}$ s; $\epsilon_0^2/\epsilon_0 = 100.0$, $\epsilon_\infty^2/\epsilon_0 = 20.0$, $\sigma_2 = 0.0$, $\tau_2 = 10^{-6}$ s.

behavior stems from the realizability requirement: $\epsilon_0^1 > \epsilon_\infty^1$ and $\epsilon_0^2 > \epsilon_\infty^2$. Depending upon the relative magnitudes of K_0, K_∞, and $K_{\text{intermediate}}$, Re[$\underline{K}_e$] may change sign up to two times. Figs. B1, *a* and *b*, depict representative behavior of the real parts of the complex permittivity and the Clausius-Mossotti function. For $\tau_1 \ll \tau_2$, as shown in Fig. B1*a*, Re[$\underline{K}_e$] can go from positive to negative and then back to positive, whereas for $\tau_1 \gg \tau_2$, as shown in Fig. B1*b*, transitions from negative to positive and then back to negative are permitted.

The single most significant observation gleaned from this example is that, for all suspension media and particles having zero DC conductivity, Re[$\underline{K}_e$] must be a monotonically decreasing function of ω, unless the suspension medium exhibits an intrinsic relaxation mechanism. This important result is a consequence of the fact that the real part of permittivity in all realizable media is a monotonically decreasing function of frequency.

Debye model with ohmic conduction

The predicted dielectrophoretic spectra are altered if DC ohmic conduction is taken into account within the suspension medium and the particle. The complex permittivities become:

$$\underline{\epsilon}_1 = \epsilon_\infty^1 + \frac{\epsilon_0^1 - \epsilon_\infty^1}{1 + j\omega\tau_1} + \frac{\sigma_1}{j\omega} \quad \text{and}$$

$$\underline{\epsilon}_2 = \epsilon_\infty^2 + \frac{\epsilon_0^2 - \epsilon_\infty^2}{1 + j\omega\tau_2} + \frac{\sigma_2}{j\omega}. \tag{B6}$$

Here, the constant σ_1 is the DC conductivity of the suspension medium and σ_2 is an effective DC conductivity of the particle. Ohmic conduction introduces Maxwell-Wagner interfacial polarization, that is, a time-dependent accumulation of free electrical charge due to the discontinuity in the normal component of free current density at the particle/liquid interface. This mechanism contributes an additional first-order relaxation process to the system. In Eq. B6, note how the conductivity dominates as $\omega \to 0$, making the imaginary part of both liquid and particle permittivities large and negative. As a consequence, the low-frequency limit of Re[$\underline{K}_e$] is always controlled by DC conduction.

$$\text{Re}[\underline{K}_e]|_{\omega \to 0} = K_0 \to \frac{\sigma_2 - \sigma_1}{\sigma_2 + 2\sigma_1}. \tag{B7}$$

With Maxwell-Wagner polarization added as an additional relaxation mechanism, there are now three distinct relaxation time constants: τ_1, τ_2, and τ_{MW}. If $\tau_{MW} \gg \tau_1, \tau_2$, then

$$\tau_{MW} = \frac{\epsilon_0^2 + 2\epsilon_0^1}{\sigma_2 + 2\sigma_1}. \tag{B8}$$

The situation becomes more complicated by the introduction of this new relaxation process because there are now six possible orderings of the relaxation times to consider. To simplify the discussion, we limit attention to the case $\sigma_1 \gg \sigma_2$, which is generally appropriate for protoplasts, due to the highly insulating nature of the membrane. In this case, it becomes clear that the low-frequency limit of the Clausius-Mossotti function becomes $K_0 \approx -0.5$. As before, investigations of the influence of critical parameters on the DEP spectrum of the particle are facilitated by making the assumption that the relaxation processes are widely separated in the frequency domain. The special cases identified and discussed below are depicted in Fig. B2, *a* through *d*. The parameter values used to obtain these plots are chosen for their illustrative value and, except for the condition $\sigma_1 \gg \sigma_2$, do not represent models for cells.

(case a') $\tau_1 \ll \tau_2 \ll \tau_{MW}$: In this case, negative DEP reigns at low frequencies and, as the frequency ω is raised, the sign of Re[$\underline{K}_e$] can change repeatedly as shown in Fig. B2 *a*.

(case b') $\tau_2 \ll \tau_1 \ll \tau_{MW}$: Here again, negative DEP reigns at low frequencies and, as the frequency ω is raised, the sign of Re[$\underline{K}_e$] can change repeatedly as shown in Fig. B2 *b*.

For both *cases a'* and *b'*, if the suspension medium exhibits no intrinsic relaxation, then Re[$\underline{K}_e$] will be a monotonically decreasing function of ω for $\omega \gg (\tau_{MW})^{-1}$. Furthermore, note that, as long as $\sigma_2 < \sigma_1$, it is not possible to achieve a positive DEP response at the lowest frequencies, due to the dominance of ohmic conduction.

(case c) $\tau_1 \ll \tau_{MW} \ll \tau_2$: In this case, τ_{MW} is calculated using the replacement $\epsilon_0^2 \to \epsilon_\infty^2$ in Eq. B8. When τ_2 is larger than τ_{MW}, the intrinsic relaxation process associated with the particle is unobservable in Re[$\underline{K}_e$] because it is swamped out by DC conduction. The implication for a protoplast is that the membrane-capacitance-dependent relaxation will not be observed. Refer to Fig. B2 *c*.

(case d) $\tau_2 \ll \tau_{MW} \ll \tau_1$: In this case, τ_{MW} is calculated using the replacement $\epsilon_0^1 \to \epsilon_\infty^1$ in Eq. B8. Now, DC conduction swamps out any influence of the intrinsic dielectric relaxation in the suspension liquid upon the dielectrophoretic effect. Refer to Fig. B2 *d*.

If τ_{MW} is the smallest of the relaxation times, then Maxwell-Wagner polarization dominates in Re[$\underline{K}_e$] and, in effect, the DC conduction suppresses any influence of intrinsic dielectric relaxation upon dielectrophoresis. Re[$\underline{K}_e$] will exhibit only a low-frequency limit K_0, given by Eq. B7, and a high-frequency limit K_∞, given by Eq. B3.

Conclusions

(*a*) For a particle in a medium with no dielectric losses, Re[$\underline{K}_e$] can not increase with increasing frequency, once it starts to decrease. This is true whether or not the particle or suspension medium exhibits ohmic DC conduction loss. (*b*) If the suspension medium does exhibit dielectric relaxation, then, at AC frequencies above those associated with any intrinsic relaxation processes in the suspension medium and above the Maxwell-Wagner polarization frequency of the particle/liquid interface, Re[$\underline{K}_e$] must be a monotonically decreasing function of ω. (*c*) Bulk conductivity in the suspension medium and/or the particle can swamp out the effect upon $\underline{K}_e$ of intrinsic relaxations associated with either the medium or the particle.

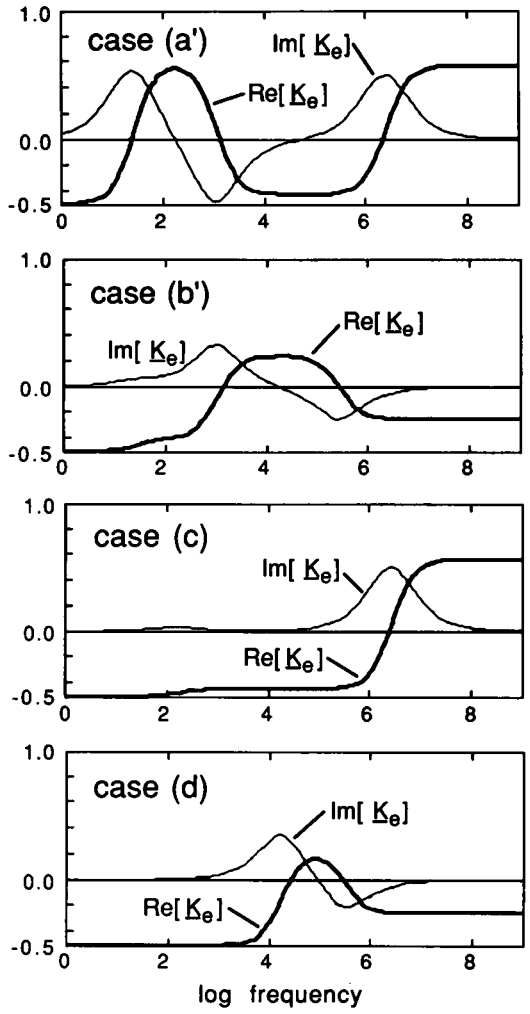

FIGURE B2 DEP spectra for lossy particles in lossy suspension media having DC conductivity σ_1 for various orderings of the relaxation time constants τ_1, τ_2, and τ_{MW}. Note that, in all cases, DC conduction dominates at the lowest frequencies, that is, $Re[\underline{K}_e] = K_0$ as defined by Eq. B7. When $\tau_2 \gg \tau_{MW}$, the intrinsic relaxation process of the particle is unobservable in $Re[\underline{K}_e]$ because it is swamped out by DC conduction; when $\tau_1 \gg \tau_{MW}$, DC conduction swamps out any influence of the intrinsic dielectric relaxation in the suspension liquid. (*a*) $\tau_1 \ll \tau_2 \ll \tau_{MW}$: $\epsilon_0^1/\epsilon_0 = 100.0$, $\epsilon_\infty^1/\epsilon_0 = 2.0$, $\sigma_1 = 10^{-6}$ *S/m*, $\tau_1 = 10^{-6}$ s; $\epsilon_0^2/\epsilon_0 = 1000.0$, $\epsilon_\infty^2/\epsilon_0 = 10.0$, $\sigma_2 = 0.0$, $\tau_2 = 10^{-3}$ s. (*b*) $\tau_2 \ll \tau_1 \ll \tau_{MW}$: $\epsilon_0^1/\epsilon_0 = 500.0$, $\epsilon_\infty^1/\epsilon_0 = 50.0$, $\sigma_1 = 10^{-6}$ *S/m*, $\tau_1 = 10^{-3}$ s; $\epsilon_0^2/\epsilon_0 = 100.0$, $\epsilon_\infty^2/\epsilon_0 = 20.0$, $\sigma_2 = 0.0$, $\tau_2 = 10^{-6}$ s. (*c*) $\tau_1 \ll \tau_{MW} \ll \tau_2$: $\epsilon_0^1/\epsilon_0 = 100.0$, $\epsilon_\infty^1/\epsilon_0 = 2.0$, $\sigma_1 = 10^{-4}$ *S/m*, $\tau_1 = 10^{-6}$ s; $\epsilon_0^2/\epsilon_0 = 1000.0$, $\epsilon_\infty^2/\epsilon_0 = 10.0$, $\sigma_2 = 0.0$, $\tau_2 = 10^{-3}$ s. (*d*) $\tau_2 \ll \tau_{MW} \ll \tau_1$: $\epsilon_0^1/\epsilon_0 = 500.0$, $\epsilon_\infty^1/\epsilon_0 = 50.0$, $\sigma_1 = 10^{-4}$ *S/m*, $\tau_1 = 10^{-3}$ s; $\epsilon_0^2/\epsilon_0 = 100.0$, $\epsilon_\infty^2/\epsilon_0 = 20.0$, $\sigma_2 = 0.0$, $\tau_2 = 10^{-6}$ s.

Discussion

Though the special cases examined above are based on a relatively simple cell model with a single inherent relaxation process, the conclusions reached are more general. For example, the protoplast can be represented by a homogeneous particle with complex permittivity in the Debye form, that is, Eq. B1. Furthermore, additional relaxations associated with more complex cell models (e.g., a protoplast with a large chloroplast inside the cytoplasm) can be added and yet the essential features of the behavior of $Re[\underline{K}_e]$ will not be changed. Similarly, DC surface conduction σ_Σ, which could influence the effective value of σ_2, can be taken into account in a cell of radius R by the following transformation: $(\sigma_2)_{eff} = \sigma_2 + 2\sigma_\Sigma/R$. One might propose a relaxation process significantly influencing $(\sigma_2)_{eff}$ in the low-frequency regime, but such a relaxation could not result in positive DEP at the lowest frequencies because realizability dictates that effective conductivity be a monotonically increasing function of frequency as long as the relaxation mechanism is first-order. Therefore, in the case of a protoplast with insulating membrane suspended in a liquid having no intrinsic relaxation process, we should expect negative DEP at the lowest frequencies.

Based on the relationship of dielectrophoretic and electrorotational spectra (Jones and Kaler, 1990), the above observations may be extended to determine the allowable rotational peaks for particles in realizable media. For example, once $Re[\underline{K}_e]$ becomes a monotonically decreasing function of ω, then only positive rotational peaks can be expected.

We are grateful to Dr. M. Moloney of the University of Calgary, for his helpful suggestions in the preparation and handling of *Canola* protoplasts, and to Professor Kenneth A. Foster of the University of Pennsylvania, who made very useful comments on the manuscript. This work was supported by grants from the National Research Council of Canada (No. 4970) and the North Atlantic Treaty Organization (NATO CRG. No. 900223).

Received for publication 16 December 1991 and in final form 9 March 1992.

REFERENCES

Arnold, W. M., H. P. Schwan, and U. Zimmermann. 1987. Surface conductance and other properties of latex particles measured by electrorotation. *J. Phys. Chem.* 91:5093–5098.

Bahaj, A. S., and A. G. Bailey. 1979. Dielectrophoresis of small particles. *In* Proceedings of the Industry Applications Society (IEEE). 1979 Annual Meeting, Cleveland, OH. 154–157.

Burt, J. P. H., R. Pethig, R. C. Gascoyne, and F. F. Becker. 1990. Dielectrophoretic characterization of *Friend* murine erythroleukaemic cells as a measure of induced differentiation. *Biochim. Biophys. Acta.* 1034:93–101.

Chizmadzhev, Y. A., P. I. Kuzmin, and V. P. Pastushenko. 1985. Theory of the dielectrophoresis of vesicles and cells. *Biol. Membr.* 2:1147–1161.

Coster, H. G. L., and J. R. Smith. 1974. The effect of pH on the low frequency capacitance of the membranes of *Chara cerallina*. *In* Membrane Transport in Plants. U. Zimmermann and J. Dainty, editors. Springer Verlag, Heidelberg. 154–161.

Foster, K. A., F. A. Sauer, and H. P. Schwan. 1992. Electrorotation and levitation of cells and colloidal particles. *Biophys. J.* In press.

Gimsa, J., P. Marszalek, U. Loewe, and T. Y. Tsong. 1991. Dielectrophoresis and electrorotation of *Neurospora* slime and murine myeloma cells: inadequacy of the single-shell model. *Biophys. J.* 60:749–760.

Jones, T. B., and G. W. Bliss. 1977. Bubble dielectrophoresis. *J. Appl. Phys.* 48:1412–1417.

Jones, T. B., and J. P. Kraybill. 1986. Active feed-back controlled dielectrophoretic levitation. *J. Appl. Phys.* 60:1247–1252.

Kaler, K. V. I. S., and T. B. Jones. 1990. Dielectrophoretic spectra of single cells determined by feedback-controlled levitation. *Biophys. J.* 57:173–182.

Marszalek, P., J. J. Zielinski, and M. Fikus. 1989. Experimental verification of a theoretical treatment of the mechanism of dielectrophoresis. *Bioelectrochem. Bioenerg.* 22:289–298.

Morikawa, H., Y. Ichikawa, M. Senda, Y. Yamada, and F. Sato. 1982.

Surface charge characteristics of mesophyll and cultured cell protoplasts. *In* Plant Tissue Culture. Maruzen Co. Ltd., Tokyo. 625–626.

Nagata, T., and G. Melchers. 1978. Surface charge of protoplasts and their significance in cell-cell interaction. *Planta.* 142:235–238.

Obi, I., Y. Ichikawa, R. Nonaka, T. Kakutani, and M. Senda. 1989. Electrophoretic studies on plant protoplasts. II. Relative amounts of various charged groups on the surface of barley mesophyll protoplasts. *Plant Cell Physiol.* 30:759–764.

O'Brien, R. W., and L. R. White. 1978. Electrophoretic mobility of a spherical colloidal particle. *J. Chem. Soc. Faraday Trans.* 74:1607–1626.

Sauer, F. A. 1983. Forces on suspended particles in the electromagnetic field. *In* Coherent Excitations in Biological Systems. H. Frölich and K. Kremer, editors. Springer Verlag, Berlin. 134–144.

Schurr, J. M. 1964. On the theory of dielectric dispersion of spherical colloidal particles in electrolyte solution. *J. Phys. Chem.* 68:2407–2413.

Schwarz, G. 1962. A theory of the low-frequency dielectric dispersion of colloidal particles in electrolyte solutions. *J. Phys. Chem.* 66:2636–2642.

Senn, A., and P. E. Pilet. 1981. Electrophoretic mobility, zeta potential and surface charges of maize root protoplasts. *Z. Pflanzenphysiol.* 102:19–32.

Tombs, T. N., and T. B. Jones. 1991. Digital dielectrophoretic levitation. *Rev. Sci. Instrum.* 62:1072–1077.

Veas, F., and M. J. Schaffer. 1969. Stable levitation of a dielectric liquid in a multi-frequency electric field. *In* Proceedings of the International Symposium on Electrohydrodynamics. Cambridge, MA. 113–115.